

# Alfred Bader Award Address in Bioinorganic or Bioorganic Chemistry

## Functional Analogs of Heme Protein Active Sites<sup>†</sup>

James P. Collman

Department of Chemistry, Stanford University, Stanford, California 94305-5080

Received August 15, 1997<sup>⊗</sup>

This article summarizes my research in biomimetic chemistry on the design and study of functional models for the active sites of metalloproteins such as hemoglobin, myoglobin, and cytochrome *c* oxidase. Particular emphasis is placed on the results which have shed light on aspects of biological systems hidden from view by the large protein components of the biological molecules. This account was presented in the form of a lecture at the ACS National Meeting, San Francisco, April 1997. The lecture was given in acceptance of the Alfred Bader Award in Bioinorganic or Bioorganic Chemistry.

This account derives from and is cast in the format of a lecture I presented in April 1997 at the ACS National Meeting in San Francisco, in recognition of the Alfred Bader Award in Bioinorganic or Bioorganic Chemistry.

I am especially pleased to acknowledge Alfred Bader, who has founded this award which recognizes the combination of organic, inorganic, and biological chemistry. It is a special privilege to be associated with an award funded by such a respected scientist as Alfred.

Table 1 lists my students, postdoctoral associates, and collaborators who, over the past 35 years, have contributed to my research program in biomimetic chemistry. These individuals are collected in groups reflecting their status at the time they joined in my work. For lack of space, I will not herald every individual, but many appear in references given in this paper. Needless to say, the hard work and intellectual contributions of these co-workers and collaborators made possible the research program recognized by this award. Even though I am credited for this research, my principal role has been that of a detached advisor.

My research program in biomimetic chemistry has been focused on the creation and study of functional analogues of metalloprotein active sites. This research began in Chapel Hill, NC, with the invention of cobalt(III) complexes<sup>1,2</sup> which selectively but stoichiometrically hydrolyze the amide bond at the terminal residue of peptides. This remarkable reaction occurs at physiological pH, near room temperature, forming stable chelated amino acid complexes. This initial work was largely carried out by my postdoctoral associate David Buckingham,<sup>3</sup> who later continued this research at The Australian



James P. Collman was born in Beatrice, NE, in 1932 and received B.S. and M.S. degrees from the University of Nebraska in 1954 and 1956 and then a Ph.D. from the University of Illinois in 1958 under the supervision of R. C. Fuson. From 1958 to 1967, he was on the faculty of The University of North Carolina at Chapel Hill; in 1967, he moved to Stanford University, where he is Daubert Professor of Chemistry. His research interests are very broad, extending across inorganic and organic chemistry but also including superconductivity. His principal research is directed toward the invention and study of functional synthetic mimics of heme protein active sites. His work has been recognized by many awards, the most recent being the American Society Alfred Bader Award in Bioinorganic or Bioorganic Chemistry, 1997. He has been a member of the National Academy of Sciences since 1975.

National University in collaboration with Alan Sargeson; together they elucidated the two mechanisms I had originally proposed for this metal-assisted peptide hydrolysis. My student Eiichi Kimura further developed this system so that one could form as well as break peptide bonds.<sup>4</sup>

<sup>†</sup> This paper is based on the address for the 1997 ACS Alfred Bader Award in Bio-inorganic or Bioorganic Chemistry presented as paper INOR 342 at the 213th ACS National Meeting of the American Chemical Society, San Francisco, CA, April 15, 1997.

<sup>⊗</sup> Abstract published in *Advance ACS Abstracts*, October 15, 1997.

(1) Collman, J. P.; Buckingham, D. A. *J. Am. Chem. Soc.* **1963**, *85*, 3039–3040.  
(2) Buckingham, D. A.; Collman, J. P.; Happer, D. A. R.; Marzilli, L. G. *J. Am. Chem. Soc.* **1967**, *89*, 1082–1087.

(3) Sutton, P. A.; Buckingham, D. A. *Acc. Chem. Res.* **1987**, *20*, 357–364.

Protein	Axial ligand	Function
Hemoglobin	His	Transport of O <sub>2</sub> Hb + 4 O <sub>2</sub> = Hb(O <sub>2</sub> ) <sub>4</sub>
Myoglobin	His	Storage of O <sub>2</sub> Mb + O <sub>2</sub> = Mb(O <sub>2</sub> )
Cytochrome P-450	Cys <sup>-</sup>	Oxidation of Substrates RH + O <sub>2</sub> + 2e <sup>-</sup> + 4H <sup>+</sup> → ROH + H <sub>2</sub> O
Cytochrome c Oxidase	His <sup>-</sup>	Reduction of O <sub>2</sub> O <sub>2</sub> + 4e <sup>-</sup> + 4H <sup>+</sup> → 2 H <sub>2</sub> O

\* Also includes Cu(I) site.

**Figure 1.** Transport, storage, and O<sub>2</sub>-reducing heme proteins.

**Table 1.** Co-Workers in Biomimetic Chemistry

Graduate Students		Post Docs & Visiting Scholars		Undergraduates
C. E. Barnes	C. Kellen-Yuen	S. Böhle	J. Marchon	G. Baird
S. Bencosme	K. Kim	B. Boitrel	L. McElwee-White	K. Doxsee
J. Brauman	E. Kimura	D. Buckingham	T. Michida	M. Eubanks
L. Chng	T.K. Kodadek	T. Chong	Y. Naruta	J. Galanter
J. Dawson	V. Lee	T. Collins	R. Oakley	B. Iverson
P. Denicovich	M. Marrocco	T. Eberspacher	R. Pettman	J. Kouba
M. Ennis	S. Raybuck	M. Elliot	M. Rapta	B. Miller
J. P. Fitzgerald	E. Schmittou	E. Evitt	C. Reed	L. Papazian
L. Fu	J. Sessler	T. Hagashi	W. Robinson	<b>Faculty</b>
R. Gagne	T. Sorrell	S. Hayes	E. Rose	J. I. Brauman
S. Groh	A. Straumanis	P. Hayoz	H. Tanaka	S. Boxer
Y. Ha	K. Suslick	R. Hembre	B. Tovrog	F. Diederich
T. Halbert	D. Tyvoll	G. Jameson	E. Uffelman	J. Ibers
P. Hampton	P. Wagenknecht	Y. Konai	K. Wong	R. Murray
N. Hendricks	X. Zang	M. L'Her		C. Reed
P. Herrmann	A. Zingg	C. Leidner		
J. Hutchison		M. Lopez		

**Table 2.** Recent Collaborators

At Stanford	Collaborators
B. Boitrel <sup>(a)</sup>	S. Boxer
L. Chng	J. I. Brauman
T. Eberspacher	R. Murray <sup>(e)</sup>
L. Fu	C. Reed <sup>(c)</sup>
P. Herrmann	E. Williams <sup>(d)</sup>
D. Tyvoll	a Dijon.
Z. Wang	b Penn State.
X. Zhang <sup>(b)</sup>	c U.S.C.
	d UC-Berkeley.
	e U.N.C.

Upon leaving Chapel Hill, I abandoned metal-activated peptide chemistry and turned my attention to the binding and activation of dioxygen by functional analogues of heme protein active sites. This work is the focus of the present account. Table 2 lists those students and collaborators who have contributed to my recent research on these functional hemoprotein mimics.

Figure 1 summarizes various roles of heme protein sites in the transport, storage, activation, and reduction of dioxygen. It is remarkable that the interaction of diverse proteins with hemes (iron complexes of porphyrins such as protoporphyrin IX) could carry out so many different functions. As we have learned, these differences derive from the axial ligands provided by ancillary groups of the protein and from the nature of the pockets on either side of the porphyrin. These two arenas are created by the tertiary structures of the folded protein. Both features create different environments about the heme so that the

**Table 3.** Properties of Dioxygen in Various Oxidation States

Species	Compounds	Bond Order	Bond Distances (Å)	Bond Energy (kcal/mol)	$\nu_{O-O}$ (cm <sup>-1</sup> )
O <sub>2</sub> ( <sup>3</sup> Σ <sub>g</sub> <sup>-</sup> )	O <sub>2</sub>	2	1.21	117.2	1555
O <sub>2</sub> ( <sup>1</sup> Δ <sub>g</sub> )	O <sub>2</sub>	2	1.22	94.7	1484
O <sub>2</sub> <sup>-</sup>	KO <sub>2</sub>	1.5	1.33		1145
O <sub>2</sub> <sup>2-</sup>	Na <sub>2</sub> O <sub>2</sub>	1	1.49	48.8	842

interaction of iron with dioxygen can achieve an extremely wide range of chemistries. Thus, in the blood, the tetrameric hemoglobin (Hb) carries and shows cooperativity in binding dioxygen. In the tissue, the structurally similar monomer myoglobin (Mb) receives dioxygen from hemoglobin and stores it for eventual reduction to water by cytochrome *c* oxidase (CcO) in the mitochondria. As indicated in Figure 1, there are similar coordination environments about iron in the three oxygen-binding hemes at the active sites of Hb, Mb, and CcO. All three hemes have on their proximal side a single axial ligand, an imidazole derived from a histidine residue. The opposite (distal) side, where oxygen binding takes place, has no axial ligand, but some amino acid residues sculpt a distal pocket which is favorable for oxygen binding and in the case of CcO provides a redox-active copper which promotes further oxygen reduction. Figure 1 also shows the oxygenase family, cytochrome P-450, which uses bound dioxygen as an oxygenating center. The heme in this oxygenase is bound to an unusual axial ligand, a mercaptide anion, derived from a cysteine residue. Although we have modeled aspects of the P-450 heme oxygenase family, that subject will not be discussed here. Our task has been to devise and examine synthetic iron porphyrins which, without the agency of a protein, provide similar porphyrin environments to the native enzymes. With these models, we have elicited the sort of chemistry manifest by "the real thing". This is the strategy behind our "functional biomimetic chemistry".

Before continuing, it is useful to review some fundamental aspects of dioxygen and its redox chemistry, as this subject may not be familiar to all interested readers. Table 3 displays the various states of dioxygen, their O—O bond orders, bond distances, bond strengths, and stretching frequencies.

The binding of dioxygen by a transition metal is not a simple Lewis acid/base reaction but involves electron transfer from the metal to dioxygen, forming a coordinated superoxide ion. Thus, those metal centers which bind dioxygen must be coordinatively unsaturated and must also have a redox potential favoring oxidation. The coordinated superoxide ion binds to the metal in an angular as opposed to a perpendicular fashion and usually has a partial negative charge concentrated on the terminal oxygen atom. This superoxide ligand may be stabilized by an electrophile in the distal cavity, for example, the formation of a hydrogen bond. The odd electron on the superoxide ligand can be further stabilized by forming a partial double bond to the metal, provided that an orbital of the correct symmetry on the metal is vacant or half-occupied. This form of  $\eta^1$  dioxygen coordination is further supported by the presence of a *trans* axial ligand on the proximal side of the porphyrin. Taken together, these factors explain the nature of various transition metal centers which bind dioxygen in the  $\eta^1$  fashion as illustrated in Figure 2.

The complexation of O<sub>2</sub> is also contrasted with the classical coordination of CO in Figure 2. The CO ligand prefers a coordination geometry perpendicular to the porphyrin plane and does not require oxidation of the metal. CO will not bind to first-row transition metal porphyrin complexes which have an

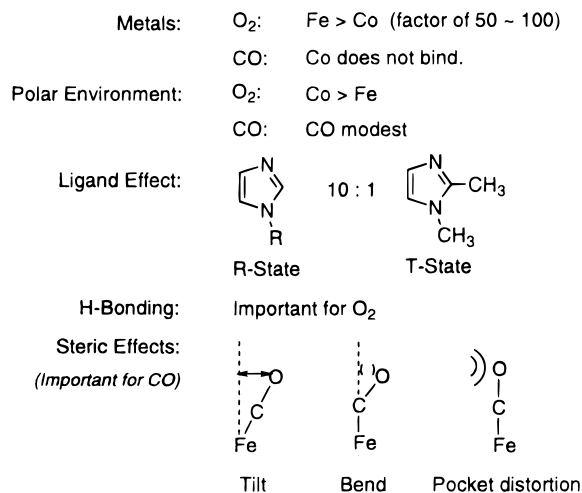


**Figure 2.** Factors which influence O<sub>2</sub>- and CO-binding affinities with metal porphyrins.

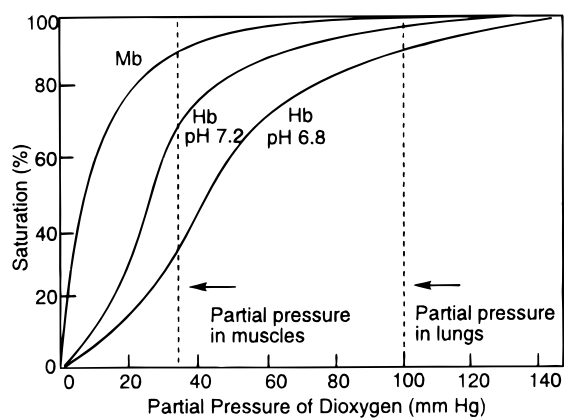


**Figure 3.** Dioxygen-affinity curves for hemoglobin (Hb) and myoglobin (Mb).

electron in the  $p_z^2$  orbital such as Co(II). Finally, it should be noted that coordinated superoxide ion is thermodynamically unstable with respect to further reduction, but such complexes may be kinetically stabilized by sheltering this sensitive ligand in a cavity such as the picket fence porphyrin provides.

The cooperative binding of dioxygen by Hb and a comparison with Mb dioxygen binding are illustrated in Figure 3. These O<sub>2</sub>-binding data reveal the sigmoid O<sub>2</sub>-binding plot for Hb and contrast that to the simple hyperbolic plot manifest by Mb. Hb and Mb work together. The relatively high concentration of dioxygen in the lungs causes Hb to pick up O<sub>2</sub> in the lungs, since Hb has a relatively high affinity at high O<sub>2</sub> concentration. In the tissues, the low O<sub>2</sub> tension causes Hb to transfer O<sub>2</sub> to Mb, since Hb develops a lower O<sub>2</sub> affinity at low O<sub>2</sub> tension as a result of the allosteric effect.

Hb cooperativity has been explained by Perutz on the basis of his discovery of two different structural forms of Hb, the high-affinity "R" state and the low-affinity "T" state (Figure 4). The low-affinity T-state is associated with a protein structure that restrains the movement of the proximal imidazole toward the porphyrin plane as iron binds dioxygen on the distal side. Recall that five-coordinate Fe(II) porphyrins (those having a single axial ligand) are high-spin and have longer bonds than the low-spin six-coordinate porphyrin complexes such as the dioxygen adduct. Restraint of the proximal axial ligand should destabilize the dioxygen adduct, lowering the affinity of the T-state for dioxygen (or for carbon monoxide).

While in my laboratory, Chris Reed prepared a simple structural model for the T-state by using an axial ligand,

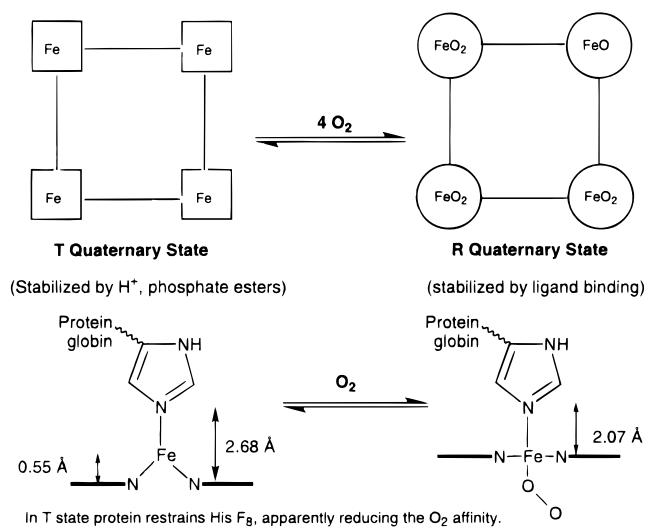


**Figure 4.** Hemoglobin cooperativity.

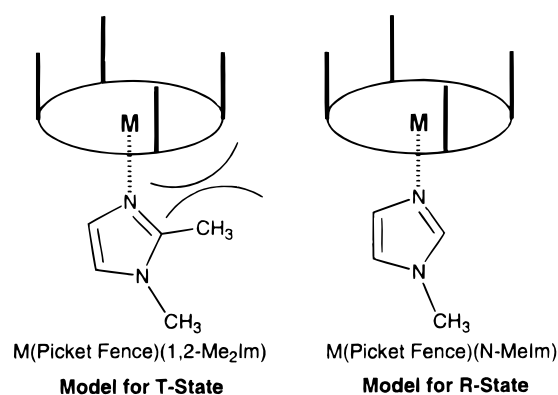


**Figure 5.** T-state versus R-state Models.

2-methylimidazole (2-MeIm).<sup>5</sup> This simple but powerful concept, illustrated in Figure 5, has been widely applied to Fe(II) porphyrin complexes. This restrained ligand, 2-MeIm, has a further virtue in that it will form only 1:1 complexes with Fe(II) porphyrins. Because of the above-mentioned spin change, most other axial ligands strongly prefer to form 2:1 complexes, since the binding affinity of the second axial ligand, leading to the low-spin state, is approximately 15 times that of the first. Throughout the present work, we have made use of Reed's T-state model.

Before discussing our recent research, I must introduce one additional facet of heme chemistry. As illustrated in Figure 6, naturally occurring hemes are enzymatically degraded such that one specific meso carbon of the porphyrin ring is converted into CO. The teleological origin of this phenomenon is unclear, but it is a general property of all hemes. This means that all oxygen-binding heme proteins must function in the presence of a low concentration of CO but O<sub>2</sub> must still be able to bind competitively. Our original "picket fence" iron porphyrin complexes<sup>6-8</sup> bind O<sub>2</sub> with an affinity similar to that of Mb, but these compounds exhibit a very much higher CO affinity.<sup>9,10</sup> A simple calculation shows that if natural systems like Hb and Mb had such a high CO affinity, they could not function in the

- (5) Collman, J. P.; Reed, C. A. *J. Am. Chem. Soc.* **1973**, *95*, 2048-2049.
- (6) Collman, J. P.; Gagne, R. R.; Halbert, T. R.; Marchon, J. C.; Reed, C. A. *J. Am. Chem. Soc.* **1973**, *95*, 7868-7870.
- (7) Collman, J. P.; Gagne, R. R.; Reed, C. A.; Halbert, T. R.; Lang, G.; Robinson, W. T. *J. Am. Chem. Soc.* **1975**, *97*, 1427-1439.
- (8) Collman, J. P. *Acc. Chem. Res.* **1977**, *10*, 265-272.
- (9) Collman, J. P.; Brauman, J. I.; Doxsee, K. M. *Proc. Natl. Acad. Sci. U.S.A.* **1979**, *76*, 6035-6039.

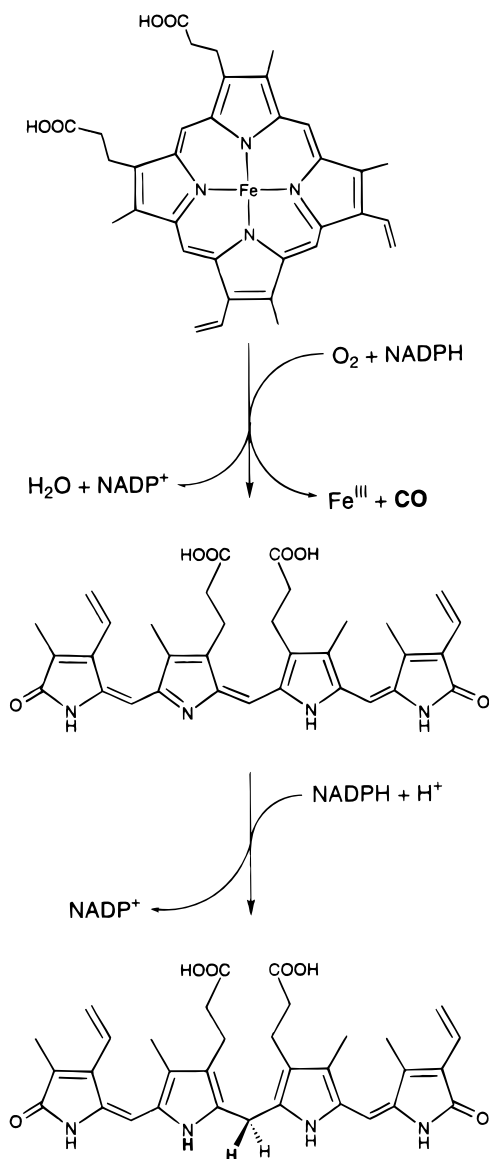


**Figure 6.** Iron salvage produces carbon monoxide.

presence of their intrinsic CO burden. We concluded that there must be a significant difference between the natural hemes and the synthetic analogues in the context of CO binding even though their O<sub>2</sub> affinities were the same. We proposed that this difference is largely steric and that it is caused by amino acid residues on the distal side (Figure 7).<sup>9,10</sup> The factors which control the relative CO/O<sub>2</sub> affinities (termed the “*M*” value) remain controversial today,<sup>11–19</sup> but I will demonstrate that steric effects can destabilize the CO ligand without changing O<sub>2</sub> affinity. H-bonding to the terminal O of the O<sub>2</sub> complexes and

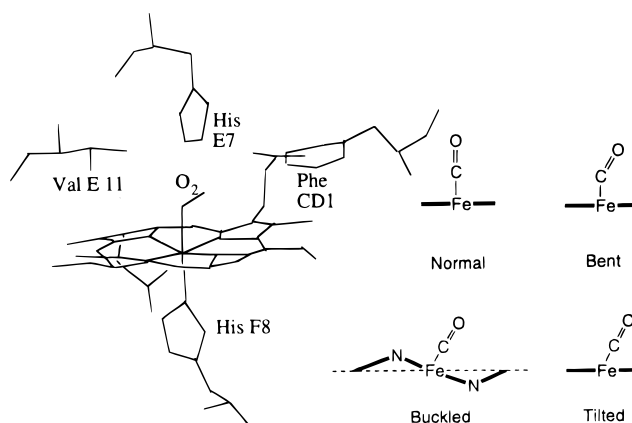


**Figure 7.** Hb and Mg active site destabilizes CO.

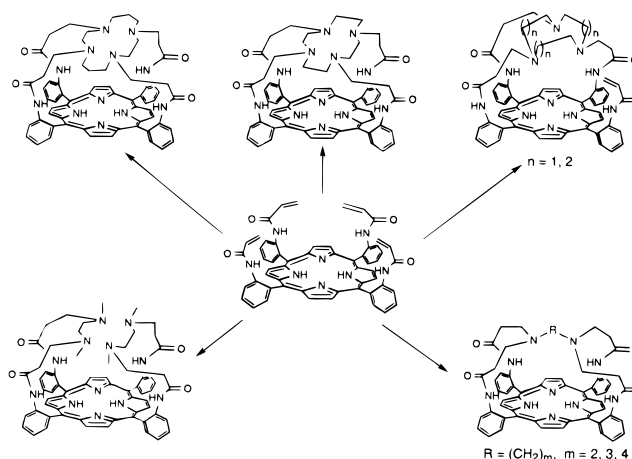


**Figure 8.** Capped porphyrins derived from the “congruent multiple Michael addition”.

polarity effects can also play a role by selectively increasing the O<sub>2</sub> affinities.

In all of our past and present work, the O<sub>2</sub> complexes of our Fe(II) porphyrins are formed reversibly and are kinetically stable at room temperature for very prolonged periods. Furthermore, these iron superoxide complexes are diamagnetic, as demonstrated by their sharp <sup>1</sup>H NMR spectra.<sup>8</sup> I would suggest that those people casually reading the literature of model Fe(II) porphyrin dioxygen binding be alert for these experimental criteria which are seldom met in practice.

Our recent work started with the discovery of an efficient new method for introducing macrocycles over one face of a porphyrin ring using a single-step, multi-Michael addition.<sup>20</sup> This congruent multi-Michael reaction is illustrated in Figure 8. A porphyrin substituted on one face with four acrylamide Michael acceptor groups is combined with various macrocyclic amines and diamines which serve as Michael donors. Without high dilution, good to excellent yields of porphyrins having a cavity over one face have been achieved using this general method. Subsequently we found that certain metal porphyrin complexes undergo more rapid multiple Michael reactions compared with free-base porphyrins. These cavity porphyrins have provided new systems to test our ideas concerning the role of steric effects on CO- versus O<sub>2</sub>-binding affinities, as well as avenues to prepare models for the unusual O<sub>2</sub>-binding site in CcO.

Our modeling has also benefited from a collaboration with Francois Diederich, who provided us with a remarkable pair of

- (10) Collman, J. P.; Brauman, J. I.; Halbert, T. R.; Suslick, K. S. *Proc. Natl. Acad. Sci. U.S.A.* **1976**, *73*, 3333–3337.
- (11) Lim, M.; Jackson, T. A.; Anfirud, P. A. *Science* **1995**, *269*, 962–966.
- (12) Quillin, M. L.; Arduini, R. M.; Olson, J. S.; Phillips, G. N. *J. Mol. Biol.* **1993**, *234*, 140–155.
- (13) Schlichting, I.; Berendz, J.; Phillips, J.; Sweet, R. M. *Nature* **1994**, *371*, 808–812.
- (14) Cheng, X.; Schoenborn, B. P. *J. Mol. Biol.* **1991**, *220*, 381–399.
- (15) Kuriyan, J.; Wilz, S.; Karpus, M.; Petsko, G. A. *J. Mol. Biol.* **1986**, *192*, 133–.
- (16) Ray, G. B.; Li, X. Y.; Ibers, J. A.; Sessler, J. L.; Spiro, T. G. *J. Am. Chem. Soc.* **1994**, *116*, 162.
- (17) Spiro, T. G. *Science* **1995**, *270*, 221.
- (18) Traylor, T. G. *Acc. Chem. Res.* **1981**, *14*, 102–109.
- (19) Traylor, T. G.; Koga, N.; Dearduff, J. A. *J. Am. Chem. Soc.* **1985**, *107*, 6504.

- (20) Collman, J. P.; Zhang, X.; Herrman, P. C.; Uffelman, E. S.; Boitrel, B.; Straumanis, A.; Brauman, J. I. *J. Am. Chem. Soc.* **1994**, *116*, 2681–2682.

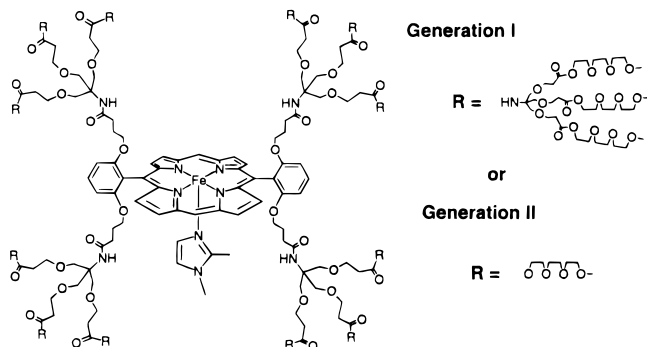


Figure 9. Dendritic porphyrins.

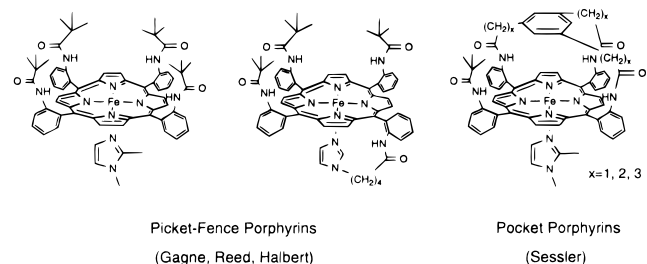
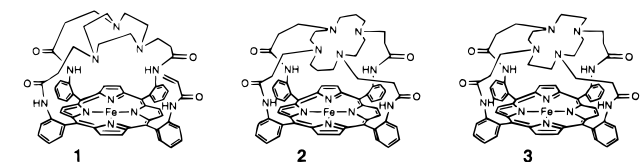


Figure 10. Picket-fence and pocket porphyrins.

Table 4. O<sub>2</sub>- and CO-Binding Data

	P <sub>1/2</sub> (torr)		M (P <sub>1/2</sub> (O <sub>2</sub> )/P <sub>1/2</sub> (CO))
	P <sub>1/2</sub> (O <sub>2</sub> )	P <sub>1/2</sub> (CO)	
Hb (T-state)	40	0.30	135
Fe (picket fence)/ (1,2-Me <sub>2</sub> Im)	38	0.0089	4280
<i>Ascaris</i>	0.002	0.1	0.02
1/(1,2-Me <sub>2</sub> Im)	2.3	2.9	0.79
2/(1,2-Me <sub>2</sub> Im)	22	> 3500	< 0.006
3/(1,2-Me <sub>2</sub> Im)	760	> 3500	< 0.22 @ 4° C
G1-Fe(II)/(1,2-Me <sub>2</sub> Im)	0.035	0.35	0.10
G2-Fe(II)/(1,2-Me <sub>2</sub> Im)	0.016	0.19	0.08



dendritic porphyrins, illustrated in Figure 9. We introduced Fe(II) into these along with a 2-MeIm axial ligand.<sup>21</sup>

In our earlier work, we had prepared Fe(II) derivatives of picket fence and pocket porphyrins. Representative examples are shown in Figure 10.

Table 4 summarizes the O<sub>2</sub> and CO equilibrium affinities of some natural heme proteins and compares these with the picket fence, macrocyclic, and dendritic porphyrins. In all cases T-state models with 2-MeIm axial ligands are used with the Fe(II) porphyrins. These affinities are displayed as P<sub>1/2</sub> values, the partial pressure at half-saturation. These P<sub>1/2</sub> values are the reciprocals of the equilibrium constants; thus a small P<sub>1/2</sub> indicates a high affinity and high P<sub>1/2</sub> a low affinity. The “M value” is also given; this is the ratio of the CO/O<sub>2</sub> affinities. M is often used by biologists to compare equilibrium bindings of these two competing gaseous ligands. Of course, a large value of M means that CO binds more tenaciously than O<sub>2</sub>. Perusing

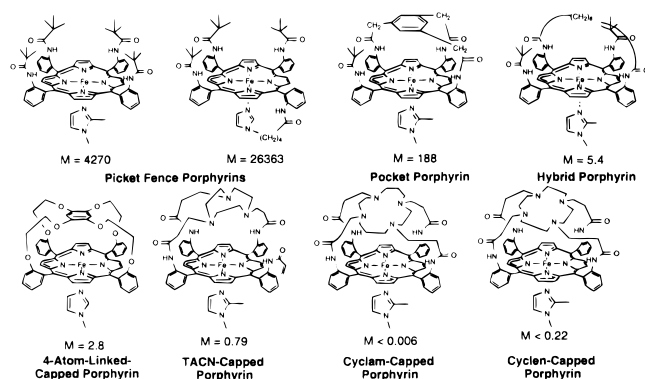


Figure 11. Dioxygen-binding myoglobin analogues.

the data in Table 4, one can see that T-state Hb has an O<sub>2</sub> affinity much like that of the T-state picket fence model but the two M values are quite different. Hb and Mb typically exhibit M values around 100, but the picket fence compounds bind CO so tenaciously that we can only estimate M as >4000! Some time ago, John Sessler showed that one pocket porphyrin exhibits an M value of about 140, not far from that of Mb. From Figure 11, one can see that the pocket and capped porphyrins are designed to distort a perpendicularly bound CO but not to interfere sterically with O<sub>2</sub>, which is intrinsically bent. As illustrated in Table 4, the new cavity porphyrins, 1–3, show dramatic reductions in M and that, in the case of 1 and 2, this difference is due to the much lower CO affinity.<sup>22</sup> In fact, these CO affinities are so low that we cannot detect CO binding in 2 and 3 at all, at 1 atm pressure. The cavity porphyrin 1, shows a low but measurable CO affinity. The O<sub>2</sub> affinities of 1 and 2 are similar to that of T-state Hb, but the sterically more demanding 3 has a much lower affinity. The M values of these new synthetic models are remarkable; they are much lower than that of the biological system, and as far as I am aware, the value measured for 2 is the lowest yet observed among model Fe(II) porphyrin complexes.

We were also pleasantly surprised by the CO- and O<sub>2</sub>-binding constants manifest by Diederich's dendrite porphyrins, G1 and G2. As shown in Table 4, these compounds have a very high O<sub>2</sub> affinity, greater than those of any of the usual heme proteins or the prior synthetic analogues.<sup>21</sup> There are some natural heme proteins which show an unusually high O<sub>2</sub> affinity; the best example is the Hb in the parasitic *Ascaris* blood worms found in pigs. The tenacious O<sub>2</sub> binding by this Hb has been something of a mystery. Some have speculated that there is a strong H-bond to the coordinated superoxide ion. The new dendrite porphyrins show an O<sub>2</sub> affinity similar to that of the estimated *Ascaris* T-state values. We speculate, from these data, that the dendrite porphyrin dioxygen complexes are stabilized by a strong H-bond, but this hypothesis must be examined by future experiments.

We have obtained structural data on the cyclam porphyrin 3 that explain its remarkably low CO affinity.<sup>22</sup> An X-ray diffraction structure of the Zn derivative of this cyclam porphyrin is shown in Figure 12. This structure shows that a CO ligand coordinated to Fe in a orientation perpendicular to the porphyrin ring would experience strong nonbonding interactions with the inner methylene H atoms, destabilizing the CO group bound to Fe. On the other hand, an intrinsically tilted O<sub>2</sub> ligand could fit within this tight cavity. This tight fit would explain the rather slow, poor, but reversible binding of O<sub>2</sub> to this Fe porphyrin.

(21) Collman, J. P.; Fu, L.; Zingg, A.; Diederich, F. *Chem. Commun.* **1997**, 193–194.

(22) Collman, J. P.; Herrmann, P. C.; Fu, L.; Eberspacher, T. A.; Eubanks, M.; Boitrel, B.; Hayoz, P.; Zhang, X.; Brauman, J. I. *J. Am. Chem. Soc.* **1997**, *119*, 3481–3489.

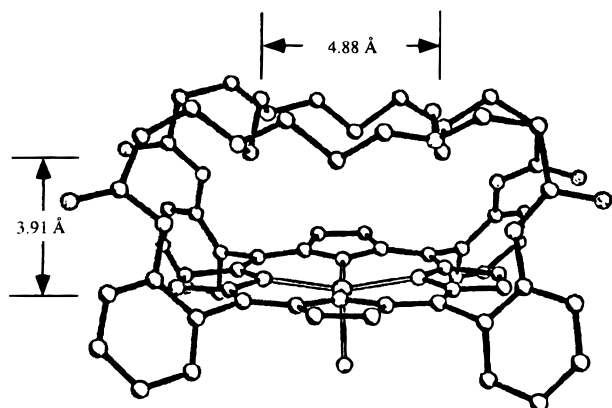


**Figure 12.** Crystal structure of cyclam-capped zinc porphyrin.

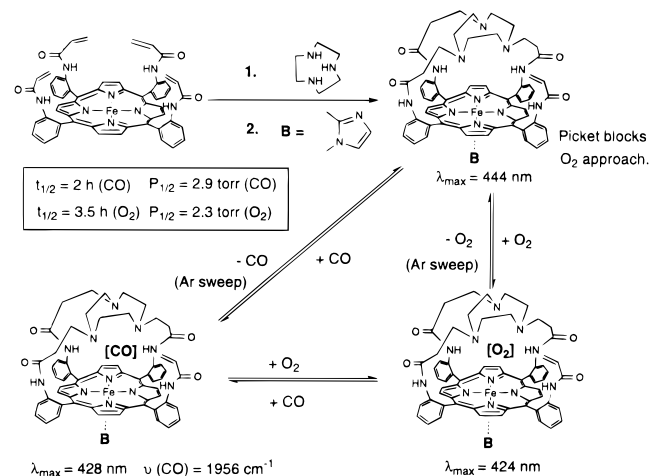


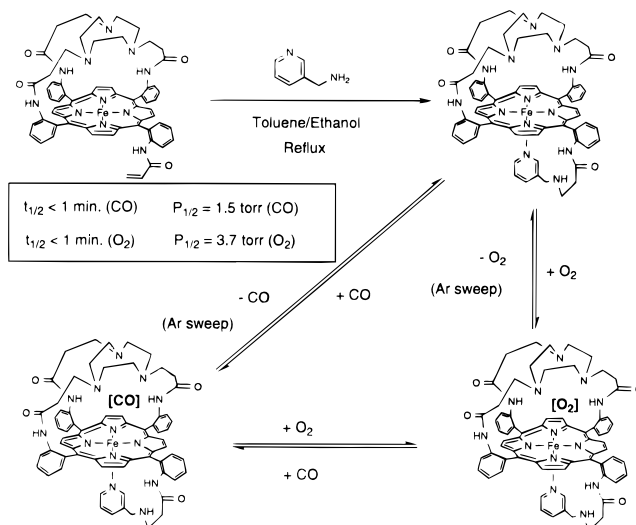
**Figure 13.** O<sub>2</sub> and CO binding to new cavity porphyrins.

I next turn to the kinetics of gaseous ligand binding to some of the new cavity porphyrins. Figure 13 shows the preparative chemistry, using the multi-Michael addition to attach triaza-cyclonane to a porphyrin previously metalated with iron. An added axial ligand binds to the proximal side. Equilibrium binding constants similar to those shown in Table 4 were found for this complex. However, the rates of CO and O<sub>2</sub> binding were discovered to be very slow, with half-lives of 2 or 3 h. Furthermore, the rate of CO binding is faster than that of O<sub>2</sub>, which is the opposite of that usually observed both with natural heme proteins and with model systems.

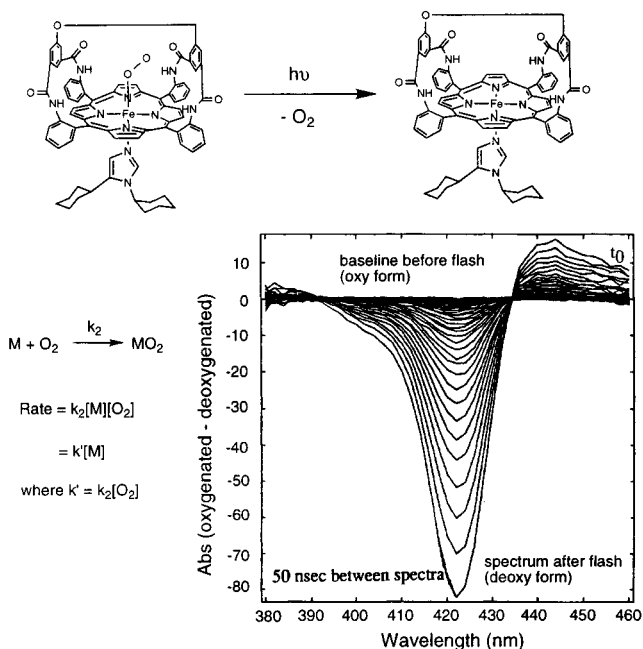
This situation was further studied with a related porphyrin shown in Figure 14. This scheme also shows a method for covalently attaching a proximal axial pyridine ligand by means of a fourth Michael addition. In this example, the rates of gaseous ligand binding were much faster; the equilibrium constants were very similar to those in Figure 13. We realized that the difference between these two systems is the presence of an acrylamide group on the distal side of the complex shown in Figure 13. This substituent partially blocks the window through which axial ligands must pass in order to bind Fe within the distal cavity. We decided to explore this hypothesis.

Figure 15 shows the kinetic profile of O<sub>2</sub> recombination after flash photolysis of a "picnic basket" porphyrin.<sup>23</sup> This reaction is very fast, but this porphyrin has two open windows to the distal cavity.

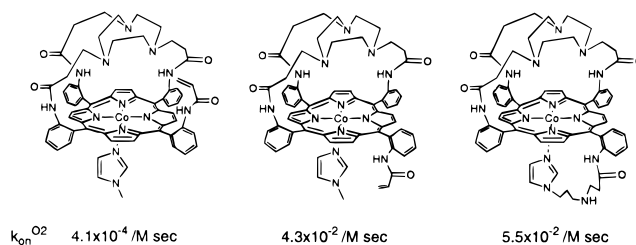
Table 5 displays both thermodynamic and kinetic data for O<sub>2</sub> binding to the above-mentioned complexes and another



**Figure 14.** O<sub>2</sub> and CO binding to tailed cavity porphyrins.



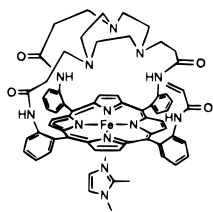
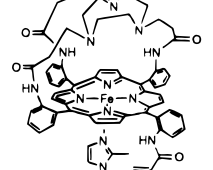
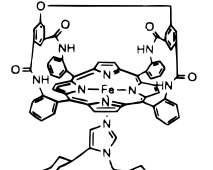
**Figure 15.** Kinetic recombination.



**Figure 16.** Impact of steric conformation on O<sub>2</sub>-binding rate constants. atropisomer in which the acrylamide substituent has been rotated to the proximal face. These data are consistent with our hypothesis that steric effects away from the O<sub>2</sub>-binding site can strongly affect the kinetics of ligand binding without influencing the equilibrium binding! As shown in Figure 16, this phenomenon does not depend on the metal; it is also seen with structurally similar Co complexes. These results should serve as a warning to those who use rate constants to estimate equilibrium constants, as has often been reported in the literature, especially for marginally stable dioxygen adducts which could only be studied by flash photolysis at low temperatures. Boxer has observed related phenomena with Mb mutants.<sup>24</sup>

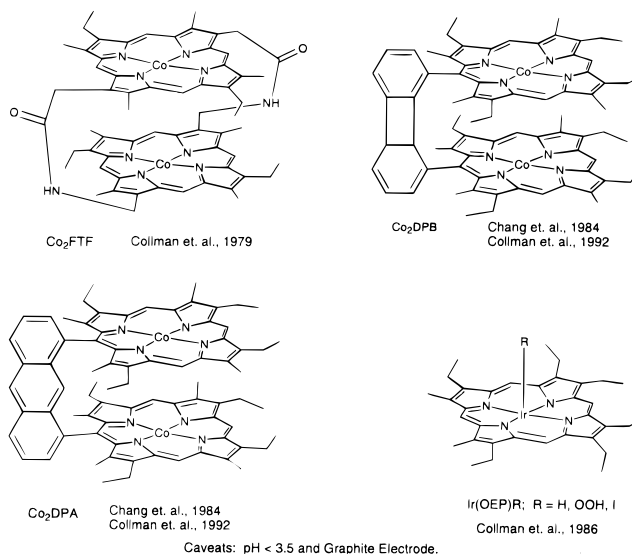
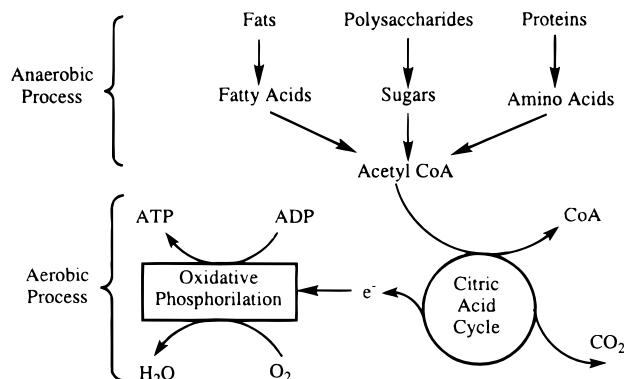
(23) Collman, J. P.; Zhang, X. M.; Wong, K.; Brauman, J. I. *J. Am. Chem. Soc.* **1994**, *116*, 6245–6251.

**Table 5.** Dioxygen-Binding Kinetics

Porphyrin	$P_{1/2O_2}$ (torr)	$K_{on}$ (M sec)
Hb (T)	40	
	140	$10^6-10^7$
Fe(Picket Fence)/ (1,2-Me <sub>2</sub> Im)	38	$10^8$ (Sessler)
	3.7	$10^{-2}$
		1
	0.28	$10^9$

I now turn to another subject, the catalytic four-electron ( $4e^-$ ) reduction of dioxygen ( $O_2$ ) to water. This reaction is catalyzed by the complex, multimetallic enzyme cytochrome *c* oxidase (CcO) in oxidative phosphorylation, which is the key step in the respiratory storage of metabolic energy as ATP. All aerobic organisms, even plants, carry out this exothermic reaction and utilize the resulting energy to keep warm and to form the universal biological currency, ATP. Fuel cells (air batteries) must conduct the same reaction at their  $O_2$ -reducing cathodes. For many years, I have been intrigued by multielectron redox catalysis. Taube introduced me to this fundamental but little studied problem when I came to Stanford 30 years ago. In Nature,  $N_2$  fixation,<sup>25</sup> photosynthetic  $O_2$  evolution, oxidative phosphorylation, and hydrogenase chemistry<sup>26</sup> all utilize metal enzyme systems to catalyze multielectron redox reactions. For many years, we have prepared and studied abiological catalysts for these chemistries. I have written two reviews<sup>27,28</sup> on this broad but obscure topic. Figure 17 displays some porphyrin complexes we<sup>29,30</sup> and others have developed to catalyze the overall  $4e^-$  reduction of  $O_2$  at graphite electrodes. These  $4e^-$  reactions typically require low pH and an edge-plane-graphite (EPG) electrode and seem to pass through a tightly bound

- (24) Balasubramanian, S.; Lambright, D. G.; Simmons, J. H.; Gill, S. J.; Boxer, S. G. *Biochemistry* **1994**, *33*, 8355–8360.  
 (25) Collman, J. P.; Hutchison, J. E.; Ennis, M. S.; Lopez, M.-A.; Guillard, R. *J. Am. Chem. Soc.* **1992**, *114*, 8074–8080.  
 (26) Collman, J. P. *Nat. Struct. Biol.* **1996**, *3*, 213–17.  
 (27) Collman, J. P.; Anson, F. C.; Bencosme, S.; Chong, A.; Collins, T.; Denisevich, P.; Exitt, E.; Geiger, T.; Ibers, J. A.; Jameson, G.; Konai, C.; Meier, K.; Oakley, R.; Pettman, R.; Schmittou, E.; Sessler, J. In *Molecular Engineering: The Design and Synthesis of Catalysts for the Rapid 4-Electron Reduction of Molecular Oxygen to Water*; Collman, J. P., et al., Eds.; Pergamon: Oxford, U.K., 1981; pp 29–45.  
 (28) Collman, J. P.; Wagenknecht, P. S.; Hutchison, J. E. *Angew. Chem., Int. Ed. Engl.* **1994**, *33*, 1537–1554.

**Figure 17.** Molecular catalysts that accomplish the  $4e^-$  reduction of  $O_2$ .**Figure 18.** Overview of metabolism.

peroxide intermediate. The EPG electrode is thought to provide some sort of axial ligand which seems required for the  $4e^-$  process.<sup>31</sup>

Before recounting our recent work, I need to outline the structure of CcO and the mechanism by which it is thought to operate. Figure 18 shows the global situation. Complex enzymatic machinery strips electrons and protons from foods (carbohydrates, proteins, and fats), leaving  $CO_2$ . These electrons are conducted to an organelle, the mitochondria, where CcO reduces  $O_2$  to water, generating heat and ATP in the course of oxidative phosphorylation. A more highly resolved view of this process is shown in Figure 19. One can see that CcO is bound in the inner matrix of the mitochondrial membrane, where  $O_2$  is reduced and protons are translocated to the outer membrane. This proton gradient is relieved by passing through another membrane-bound enzyme, ATPase, which uses this energy to make ATP from ADP and phosphate. Electrons required for the overall reduction are brought to CcO by a single-electron carrier, cytochrome *c*, which is a coordinatively saturated, low-spin heme that shuttles between the +2 and +3 oxidation states. Note that eight protons are involved in the catalytic reaction; four are used in the conversion of  $O_2$  to  $2H_2O$  and the other four are translocated to the outer membrane during the reduction.

- (29) Collman, J. P.; Denisevich, P.; Konai, Y.; Marrocco, M.; Koval, C.; Anson, F. C. *J. Am. Chem. Soc.* **1980**, *102*, 6027–6036.  
 (30) Collman, J. P.; Brauman, J. I.; Collins, T. J.; Iverson, B.; Sessler, J. L. *J. Am. Chem. Soc.* **1981**, *103*, 2450–2452.  
 (31) Collman, J. P.; Chng, L. L.; Tyvoll, D. A. *Inorg. Chem.* **1995**, *34*, 1311–1324.

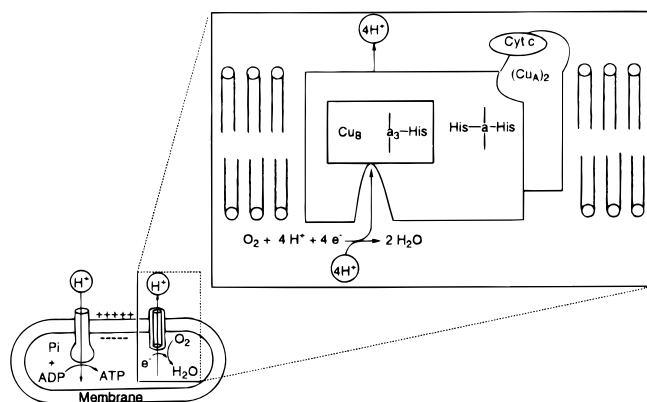


**Figure 19.** Cytochrome *c* oxidase.

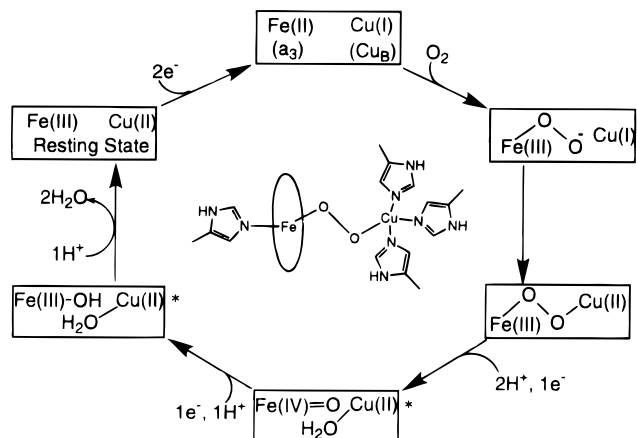


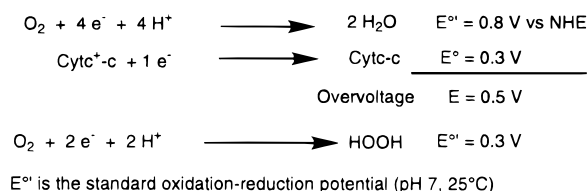
**Figure 20.** Proposed reaction cycle for the 4e<sup>-</sup> reduction of O<sub>2</sub> by cytochrome *c* oxidase.

Recently, the active sites of two cytochrome *c* oxidases were structurally characterized by X-ray diffraction.<sup>32–34</sup> These structures demonstrate that, as previously surmised from indirect evidence, the O<sub>2</sub>-binding/activating site in each CcO is composed of a Mb-like heme and a copper atom (Cu<sub>B</sub>) coordinated to three imidazoles from histidine residues on the distal side. As illustrated in Figure 19, two other metal sites, a coordinatively saturated heme and a dinuclear Cu<sub>2</sub> site, are involved in storing and transferring the electrons during the 4e<sup>-</sup> reduction.

The mechanism by which CcO effects the 4e<sup>-</sup> reduction of O<sub>2</sub> is not fully understood. Many issues remain to be resolved, particularly the role of Cu in O<sub>2</sub> binding and the nature of some of the O<sub>2</sub>-bound intermediates that may be present during the catalytic cycle. Most authors propose that the cycle passes through a peroxide intermediate—the result of two sequential 1e<sup>-</sup> reductions of O<sub>2</sub> as it interacts with Fe(II) and Cu(I), which are oxidized by 1e<sup>-</sup> each. There is disagreement as to whether the resulting peroxide is bound only to Fe or whether it bridges Fe and Cu. Figure 20 displays one proposed mechanism. Those intermediates which are believed to have been observed by time-resolved resonance Raman spectroscopy (using O isotopes) are indicated by an asterisk.

As outlined in Figure 21, we have pointed out an interesting fact consistent with a peroxide intermediate. The reduction

(a) The Overvoltage is Consistent



*E*<sup>o</sup> is the standard oxidation-reduction potential (pH 7, 25°C)

(b) Cytochrome *c* Oxidase reduces H<sub>2</sub>O<sub>2</sub>.

**Figure 21.** Arguments that peroxide is an intermediate during cytochrome *c* oxidase reduction of O<sub>2</sub>.

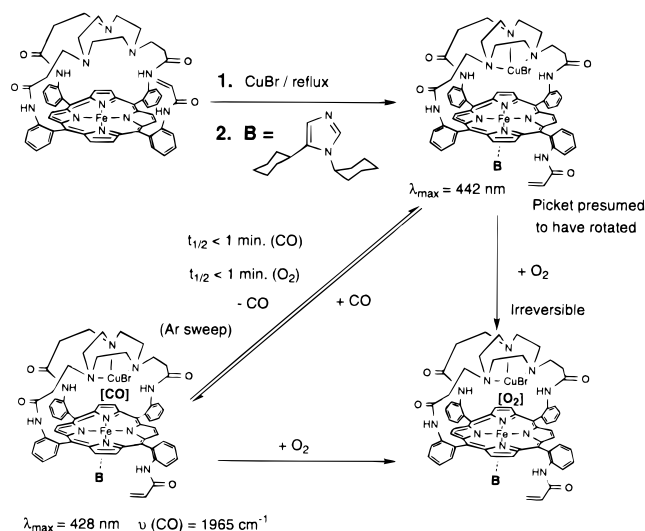


**Figure 22.** O<sub>2</sub> and CO binding to CcO model.

potential of cytochrome *c*, which is the initial reductant, is 0.3 V (vs NHE). Thus the system can be thought of as an electrochemical potentiostat set at 0.3 V. The thermodynamic potential connecting O<sub>2</sub> and H<sub>2</sub>O<sub>2</sub> at pH 7 is also 0.3 V (vs NHE). Consequently, little or no energy would be released in the formation of a peroxide intermediate. This argument assumes that the two metals bind the peroxide ligand with an affinity near that of a proton at pH 7. The overall 4e<sup>-</sup> reduction of O<sub>2</sub> at pH 7 would produce 0.8 V, which yields an overvoltage of 0.5 V for the catalytic reaction. Consistent with our point is the observation that the last two 1e<sup>-</sup> reduction steps are thought to release all of the energy during the catalytic cycle, driving the proton pump and generating heat. Interestingly, CcO is also able to reduce H<sub>2</sub>O<sub>2</sub> to H<sub>2</sub>O.

Our own experiments began with the synthesis of a model for the CcO O<sub>2</sub>-binding/activating site shown in Figure 22.<sup>35</sup> This scheme uses the multiple Michael addition of a triazacyclononane cap to a premetallated Fe porphyrin. Copper(I) is introduced, and a bulky imidazole, used in excess, coordinates to Fe(II) exclusively on the proximal face. The triazacyclononane ligand is known from Wieghardt's<sup>36</sup> and Tolman's<sup>37</sup> earlier work to support Cu in both the +1 and +2 oxidation states. Because it binds CO and O<sub>2</sub> rapidly, as shown in Figure 22, this system is thought to have the unconsummated acrylamide positioned on the proximal face. We were pleased to discover that O<sub>2</sub> binding is "irreversible", affording a diamag-

(32) Tsukihara, T.; Aoyama, H.; Yamashita, E.; Tomizaki, T.; Yamaguchi, H.; Shinzawa-Itoh, K.; Nakashima, R.; Yaono, R.; Yoshikawa, S. *Science* **1995**, *269*, 1069–1074.

(33) Tsukihara, T.; Aoyama, H.; Yamashita, E.; Tomizaki, T.; Yamaguchi, H.; Shinzawa-Itoh, K.; Nakashima, R.; Yaono, R.; Yoshikawa, S. *Science* **1996**, *272*, 1136–1144.

(34) Iwata, S.; Ostermeier, C.; Ludwig, B.; Michel, H. *Nature* **1995**, *376*, 660–669.

(35) Collman, J. P.; Herrmann, P. C.; Boitrel, B.; Zhang, X.; Eberspacher, T. A.; Fu, L. *J. Am. Chem. Soc.* **1994**, *116*, 9783–9785.

(36) Wieghardt, K. *Angew. Chem., Int. Ed. Engl.* **1989**, *28*, 1153.

(37) Mahapatra, S.; Halfen, J. A.; Wilkinson, E. C.; Pan, G.; Wang, X.; Young, V. G.; Cramer, C. J.; Que, L.; Tolman, W. B. *J. Am. Chem. Soc.* **1996**, *118*, 11555–11574.



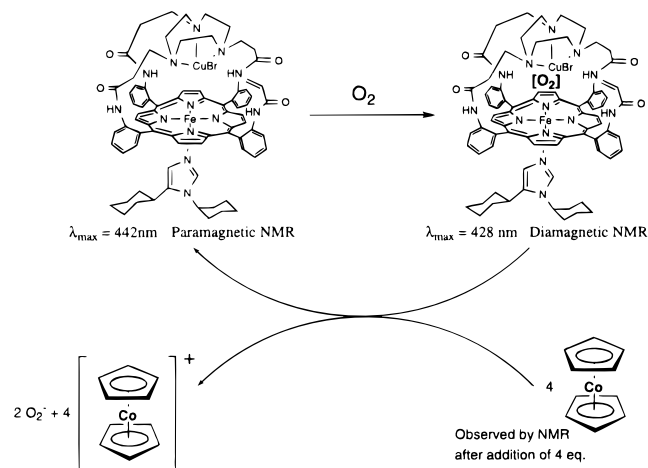


Figure 23. Redox titration.

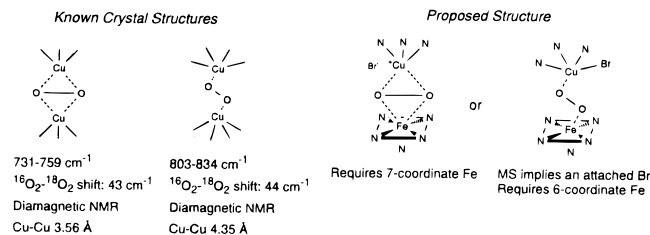
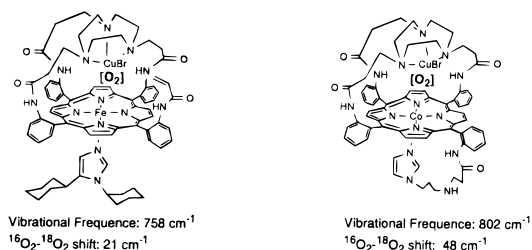


Figure 24. Raman spectroscopic studies on CcO models.

netic complex determined by  $^1\text{H}$  NMR. We believe this diamagnetism results from magnetic coupling between a low-spin Fe(III) center and Cu(II) through a peroxide bridge, as has been observed in  $(\text{Cu})_2$  oxygen carriers.

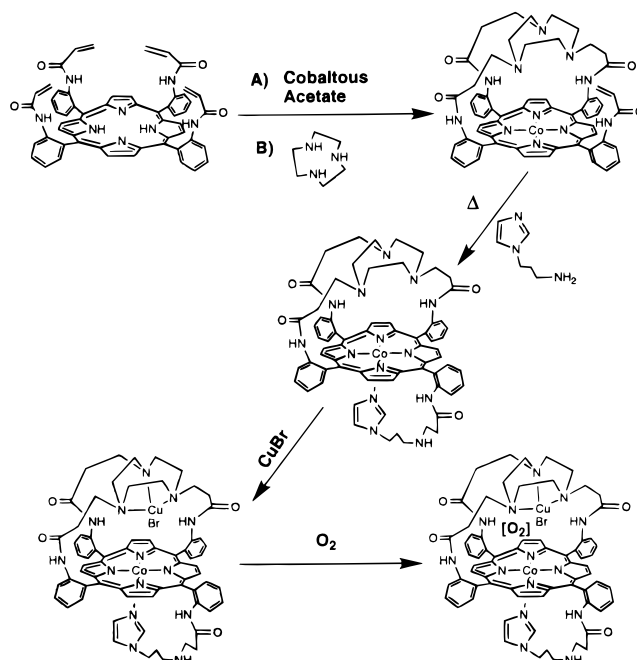
We established the nature of the peroxide ligand by a redox titration as illustrated in Figure 23. This complex takes up exactly 4 equiv of the  $1e^-$  reductant, cobaltocene ( $\text{Cp}_2\text{Co}$ ). The fully reduced system then takes up exactly 1 equiv of  $\text{O}_2$ , in a gas titration. We repeated this cycle of redox titration and  $\text{O}_2$  binding four times.

The more traditional method for characterizing a peroxide ligand is vibrational spectroscopy, using oxygen isotopes. As shown in Figure 24, our Raman studies of the peroxide adduct gave equivocal results. Although the O—O stretch was observed at a frequency which is characteristic of a peroxide group, the isotopic shift was found to be only half the predicted value. With  $^{17}\text{O}$  substitution, we uncovered evidence for vibronic coupling which could account for this abnormal isotopic shift. Later we found a Co/Cu complex to form a similar peroxide bridge upon binding  $\text{O}_2$  and to exhibit a normal isotopic shift. Figure 24 also shows vibrational frequencies for two types of structurally characterized bridging peroxides.<sup>38–40</sup> The systems we have prepared have not been structurally characterized, for

(38) Jacobson, R. R.; Tyeklar, Z.; Farooq, A.; Karlin, K. D.; Liu, S.; Zubieta, J. *J. Am. Chem. Soc.* **1988**, *110*, 3690.

(39) Kitajima, N.; Fujisawa, K.; Fujimoto, C.; Moro-oka, Y.; Hashimoto, S.; Kitagawa, T.; Tatsumi, A. *J. Am. Chem. Soc.* **1992**, *114*, 1277.

(40) Kitajima, N.; Moro-oka, Y. *Chem. Rev.* **1994**, *94*, 737.

Figure 25. Synthesis of the cytochrome *c* oxidase model.

lack of single crystals. Possible bonding modes for our peroxide complexes are also shown in Figure 24, but at present we cannot decide between these.

As shown in Figure 25, we used a similar method to prepare a Co porphyrin capped with a Cu macrocycle.<sup>41</sup> We also introduced a proximal covalent bound axial imidazole by utilizing a second Michael addition to the remaining acrylamide group under conditions which rotate the “picket” to the proximal face prior to the introducing of Cu(I) into the TACN cap. This complex also binds  $\text{O}_2$  stoichiometrically in a seemingly irreversible manner. The Raman data for this peroxide bridge were already presented in Figure 24. The precise titration results for this Co(II)/Cu(I) complex with  $\text{O}_2$  are given in Figure 26. As illustrated in Figure 27, we then carried out the same redox titration with this bridging peroxide as we had developed with the closely related Fe/Cu complex. Once more, we were able to carry out repeated stoichiometric cycles of  $\text{O}_2$  addition/ $\text{Cp}_2\text{Co}$  titration, consistent with a peroxide-bridging Co(III)/Cu(II)  $\text{O}_2$  adduct.

Finally, I turn to the question of electrocatalytic reduction of dioxygen. Rotating ring-disk voltammetry is a powerful technique for examining this electrocatalytic process. A typical apparatus is shown in Figure 28. The central electrode is an edge-plane-graphite (EPG) disk; this is surrounded by a platinum ring electrode. The two are separated by an insulating Teflon spacer. A catalyst candidate is adsorbed on the EPG electrode. A potentiostat sweeps the EPG through a range of potentials; at the same time, the Pt electrode is maintained at a high oxidizing potential. The Pt electrode serves as a sensor for  $\text{H}_2\text{O}_2$ , which may be produced in the catalytic reduction of  $\text{O}_2$  at the disk electrode. The entire assembly is rotated at a fixed velocity. This rotation helps to draw the  $\text{O}_2$ -saturated aqueous electrolyte to the electrode surface. The rate of  $\text{O}_2$  diffusion to the disk electrode is increased at higher rotation rates because the width of the stagnant layer on the disk electrode surface is decreased at faster rotational rates. The fluid mechanics of this situation have been modeled by the Levich equation.<sup>42,43</sup> By

(41) Collman, J. P.; Fu, L.; Herrmann, P. C.; Zhang, X. *Science* **1997**, *275*, 949–951.

(42) Koutecky, J.; Levich, V. G. *Zh. Fiz. Khim.* **1956**, *32*, 1565–1575.

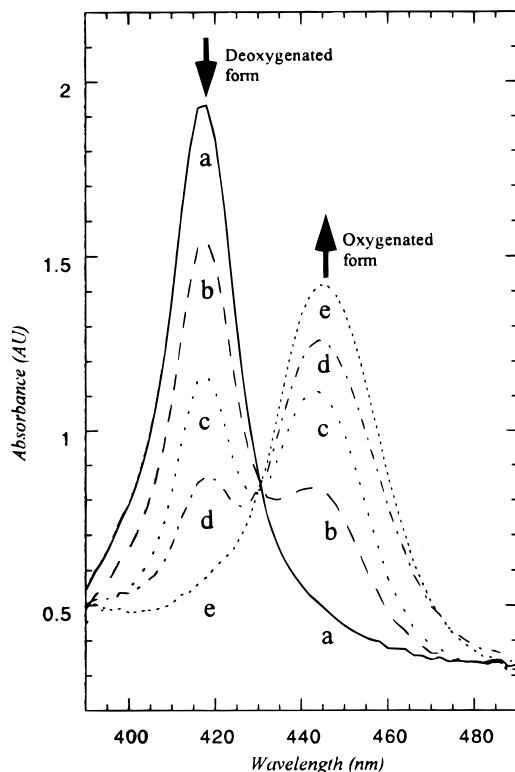


Figure 26. Dioxygen titration.

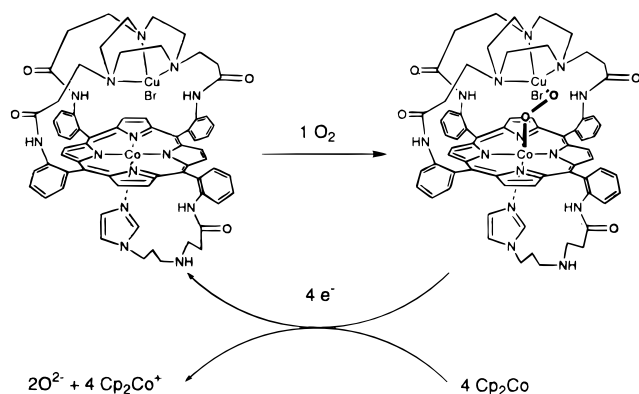


Figure 27. Redox titration.

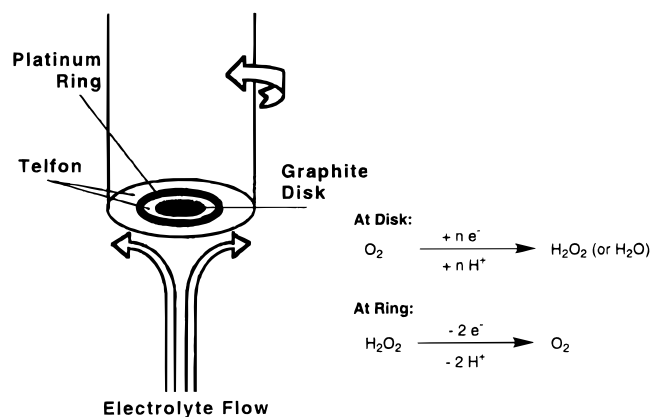


Figure 28. Rotating ring-disk electrode (RRDE) assembly.

evaluating the rotating ring-disk voltammograms over a series of rotational rates and calibrating the system with a standard redox couple, it is possible to evaluate the relative amounts of

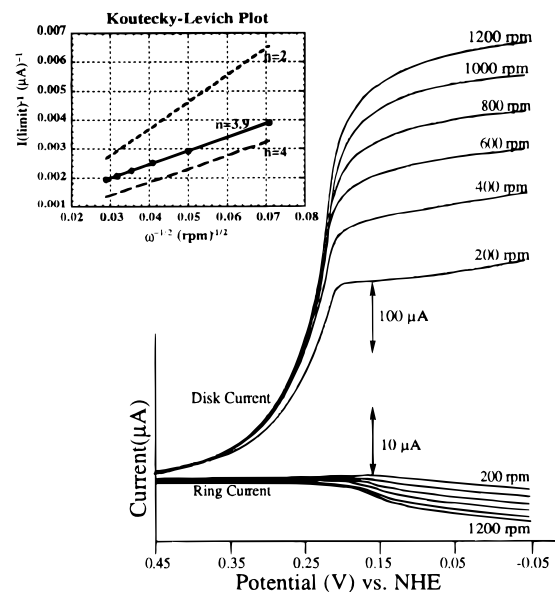


Figure 29. The  $4e^-$  reduction of  $\text{O}_2$  by the CcO model in pH 7.3 buffer.

$2e^-$  reduction to  $\text{H}_2\text{O}_2$  vis-à-vis  $4e^-$  reduction to  $\text{H}_2\text{O}$ . The  $\text{O}_2$  partial pressure and the pH of the electrolyte buffer can also be varied.

Figure 29 shows results we obtained with the Co/Cu catalyst at physiological pH (7.3).<sup>41</sup> The upper plots show the disk currents (given on the vertical coordinate) versus the potential imposed on the catalyst at various rotational rates. When a critical potential is reached, the catalytic current rises and increases to a limiting value at more reducing potentials. This plateau is raised by employing faster rotational frequencies for the electrode assembly. The corresponding reducing currents at the Pt ring electrode indicate the reduction of any  $\text{H}_2\text{O}_2$  produced at the ring. The ring currents have been amplified by a factor of 10 because they are so small. The overall result confirms a catalytic reduction of  $\text{O}_2$  at the disk presumably by a  $4e^-$  process, since very little  $\text{H}_2\text{O}_2$  is detected. This situation can be better quantified by using the reciprocal "Koutecky/Levich" plots as shown in Figure 29. The slope of this line indicates the number of electrons ( $n$ ) involved in the electrocatalytic reaction. In this case, the slope is close to 4; coupled with the very small quantity of  $\text{H}_2\text{O}_2$  detected at the Pt ring, this confirms that the Co/Cu complex catalyzes an overall  $4e^-$  reduction of  $\text{O}_2$ .

The results illustrated in Figure 29 are remarkable when considered in the context of our earlier work on metal porphyrin catalysis of  $\text{O}_2$  reduction. Our prior catalysts<sup>28</sup> showed  $4e^-$  reduction of  $\text{O}_2$  only at pH values below 3.5. We had never before been able to study catalysts fitted with a discrete axial ligand. We have found that this axial ligand is required to achieve  $4e^-$  reduction. In the present case, the redox role of the second metal, Cu(I), is obvious. The Cu(II)/Cu(I) potential is close to the potential where catalytic reduction of  $\text{O}_2$  begins; in the absence of Cu, this molecule catalyzes only the  $2e^-$  reduction of  $\text{O}_2$ . The catalyst system shown in Figure 29 closely mimics the activity of CcO itself, including the putative involvement of a peroxide intermediate in the catalytic cycle.

Cobalt is not iron, but cobalt has been used as a surrogate for iron in porphyrins which bind and reduce dioxygen. The Fe/Cu analogue of the  $4e^-$  Co/Cu catalyst shows only  $2e^-$  reduction of  $\text{O}_2$ , as do all other Fe porphyrin catalysts we examined in our prior work. We have a possible explanation for this behavior. Cyclic voltammograms of these catalysts in

(43) Levich, V. G. *Physicochemical Hydrodynamics*; Prentice-Hall: Englewood Cliffs, NJ, 1962.

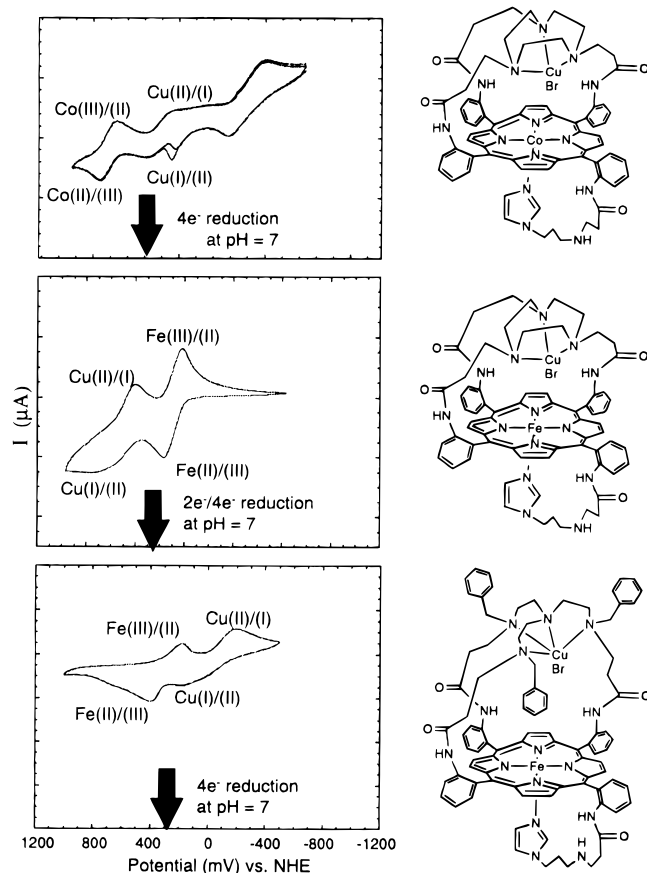


Figure 30. Cyclic voltammograms of CcO models.

the absence of  $O_2$  show that the  $Co(III)/Co(II)$  potential is higher than the  $Cu(II)/Cu(I)$  potential whereas the situation with the  $Fe/Cu$  catalyst is reversed. This would mean that the  $Cu$  center

should be reduced first, before  $Fe$ , so that  $O_2$  binding might start at the  $Cu$  center, perhaps on the outside of the porphyrin/macrocycle cavity. This could lead to a  $2e^-$  pathway with only  $Cu$  involved. On the other hand, prior reduction of the  $Co$  center would direct the  $O_2$  ligand inside this distal cavity so that it could bind to  $Cu$ , as that center is subsequently reduced. Remember that, in both cases, the proximal porphyrin face is blocked by an internally appended axial ligand.

That brings me to mention our most recent catalyst which is also shown in Figure 30. In this complex, an  $Fe$  porphyrin is fitted with a chelated axial imidazole on the proximal face and with a distal macrocyclic  $Cu$  cap (unpublished results). But this new cap is tetrapodal and should bring four nitrogen ligands to bond with  $Cu$  as compared with the three nitrogen ligands from the triazacyclononane cap we employed in the other two catalysts. Cyclic voltammograms of the three cases show that the newest catalyst has an  $Fe(III)/Fe(II)$  potential higher than the  $Cu(II)/Cu(I)$  potential; in this case,  $O_2$  is reduced by a predominately a  $4e^-$  pathway. The arrows in Figure 30 show the potential at which catalytic reduction of  $O_2$  begins. In each case, this point is between the potentials of the two redox-active metal centers, although these values are not strictly comparable because ligation by  $O_2$  will shift the potential of the metal centers. It is clear that our present understanding of these new catalysts is embryonic. Furthermore, most of these new compounds have not yet been structurally characterized. A series of new catalyst sites which are structurally closer to "the real thing" are also under construction in my laboratories.

**Acknowledgment.** Over many years, various aspects of this research have been generously supported by the National Institutes of Health and the National Science Foundation. This paper was written with help from Lei Fu.

IC971037W